ADVANCES IN HEAT TRANSFER ENHANCEMENT BY OPTICAL TECHNIQUES

Robert Tauscher, Martin Jordan, Franz Mayinger
Lehrstuhl A für Thermodynamik, Technische Universität München
D - 85747 Garching
Germany
Phone: ++49 89 289 16221, Fax: ++49 89 289 16218
e-mail: tauscher@thermo-a.mw.tu-muenchen.de

ABSTRACT

The enormous advances in computer-aided data processing enable the engineer to use optical measuring techniques for the investigation of heat and mass transfer phenomena as well as fluid dynamics. Due to the fact, that these optical methods work inertialess and non-invasive, in contrary to common techniques like probes, they will not have any disturbing influence on the phenomena to be investigated. The combination of classical optical methods with new equipment like high speed video cameras yields new experimental possibilities. In the first part of this paper an overview of optical measurement techniques is given. The second part describes the application of some of these techniques in the investigation of heat transfer, with special emphasis to heat transfer enhancement in compact heat exchangers. The expamples demonstrate the capabilities and the importance of new optical measuring techniques.

INTRODUCTION

Optical methods are used in Thermo-Fluiddynamics research since many years because of their big advantages. As they work non-invasive and inertialess they do not influence the process that has to be investigated in contrary to probes and can be used even for highly transient processes like combustion.

The development of optical methods is supported by the availability of new equipment like high energy light sources (e.g. laser), intensified electronical camera systems (e.g. CCD-cameras), and electronic devices as well as new software. This allows to reduce the time of data processing, storing and evaluating, which has been very time consuming in the past.

One can distinguish between imaging and non imaging techniques. Imaging techniques (global methods) provide simultaneous information over a larger area (commonly two-dimensional) and use any kind of conventional or electronic photographic material to store this information. Non imaging optical methods work with a measurement volume often smaller than 1 cubic millimeter, and therefore are called pointwise methods as well.

In table 1 examples for modern, optical measurement techniques to determine temperature, concentration, density, velocity and droplet size - which are mainly the interesting dimensions in Thermo-Fluiddynamics - are given. The table also informs about the physical effect of the methods, as well as the recording dimension and the application. One can see that a parameter, which is interesting in Thermo-Fluiddynamics can often be measured by various techniques. For example the velocity in a droplet spray can be measured by double-pulse holography, particle image velocimetry (PIV) or laser Doppler velocimetry (LDV). For each application a different method might be prefered. In our example, a pulse hologram contains the full three-dimensional information about the process in one moment. With PIV a two-dimensional image of the moving droplets can be recorded continuously and with LDV only (three-dimensional) velocity information in one single point is available, but with a data-rate of up to several kHz, depending on the spray.

As it is not possible to discuss all optical techniques known from the literature in detail here, emphasis is given to

- Holography
- Holographic Interferometry and

light scattering methods like

- Rayleigh scattering
- Raman scattering
- Laser-Induced Fluorescence
- Particle image-velocimetry

Some examples will show, how classical measurement-techniques like

- Self Fluorescence and the
- Toepler-Schlieren Technique

can become very interesting again with newest high speed video camera devices.

The first part of this paper will give the necessary basic explanations of the measurement techniques mentioned above. In the second part several examples will show, how some of these techniques have been used to investigate heat transfer

Measuring technique	Physical effect	Application	Dimensions
schlieren and shadowgraph	light refraction	density, temperature	2D (integ.)
holography	holography	particle size, velocity	3D
interferometry	change of light velocity	density, temperature	2D (integ.)
laser Doppler velocimetry	Mie scattering	flow velocity	point
phase Doppler	Mie scattering	particle size	point
particle image velocimetry	Mie scattering	flow velocity	2D
dynamic light scattering	Rayleigh scattering	density, temperature	point – 2D
Raman scattering	Raman scattering	mol. concentration, temperature	point – 1D
coherent anti-stokes Raman spectroscopy	CARS scattering	mol. concentration, temperature	point
laser induced fluorescence	fluorescence	concentration, temperature	point – 2D
absorption	absorption	concentration, temperature	point – 2D (integ.)
pyrometry	thermal radiation	temperature	1D
thermography	thermal radiation	temperature	2D (integ.)
self fluorescence	therm. fluorescence, chemoluminescence	concentration, temperature	2D (integ.)

TABLE 1: EXAMPLES OF OPTICAL MEASUREMENT TECHNIQUES USED IN THERMO-FLUIDDYNAMICS

phenomena, with special interest to heat transfer enhancement in compact heat exchangers.

NOMENCLATURE

e rib height, mm
D Diameter, mm
h, H height, mm
L length, m
Nu Nusselt number, dimensionless
Ma Mach number, dimensionless
p rib spacing, mm
Re Reynolds-number, dimensionless
T Temperature, °C, K
Tu turbulence intensity, dimensionless
W width, mm
x,y,z coordinates, m, cm, mm
• angle of inclination, °•
• wavelength, nm
• friction factor, dimensionless

0 smooth duct
m mean
H Heater
W Wall

OPTICAL MEASUREMENT TECHNIQUES

Holography

1949 Gabor found a new technique to record and reconstruct three-dimensional pictures, called holography (”complete recording”). But it needed the invention of the laser as a coherent light source, 10 years later to discern the large variety of this technique. The general theory of holography is so comprehensive, that for a detailed description, one must refer to the literature (Gabor, 1951, Kiemle and Röss, 1969, Mayinger, 1994). Here only the principles, necessary for understanding the holographic measurement technique can be mentioned.

The principles of holography can be explained by comparing this measurement technique with conventional photography. Figure 1 shows an ordinary photography of an object, represented by three single object points P1, P2, P3. By choosing a camera position, a fixed perspective will occur. This is shown by the different position of the (more or less sharp) projected picture points in the focal planes B-B. Holography avoids the disadvantage of a fixed perspective and a limited depth of sharpness. The main idea of the principle is, to store the whole wave field, emerging out of the object in the hologram-plane H-H. Figure 2 shows the principle of storing the phase of a wave. The

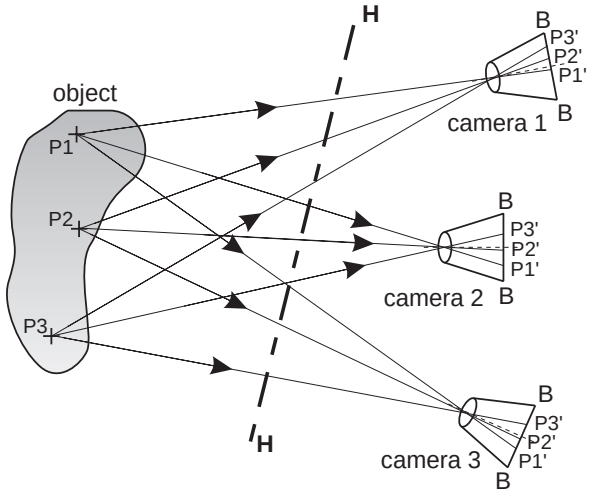

FIGURE 1: CAMERA POSITIONS (1, 2, 3) AND PERSPECTIVE. ONE HAS TO PAY ATTENTION TO THE DIFFERENT LENGTH OF THE RAYS AND THE DIFFERENT POSITION OF THE PICTURE POINTS P1′, P2′ AND P3′. THE VARIABLE PLANE H-H WILL BE CALLED ”HOLOGRAPHIC-PLANE”.

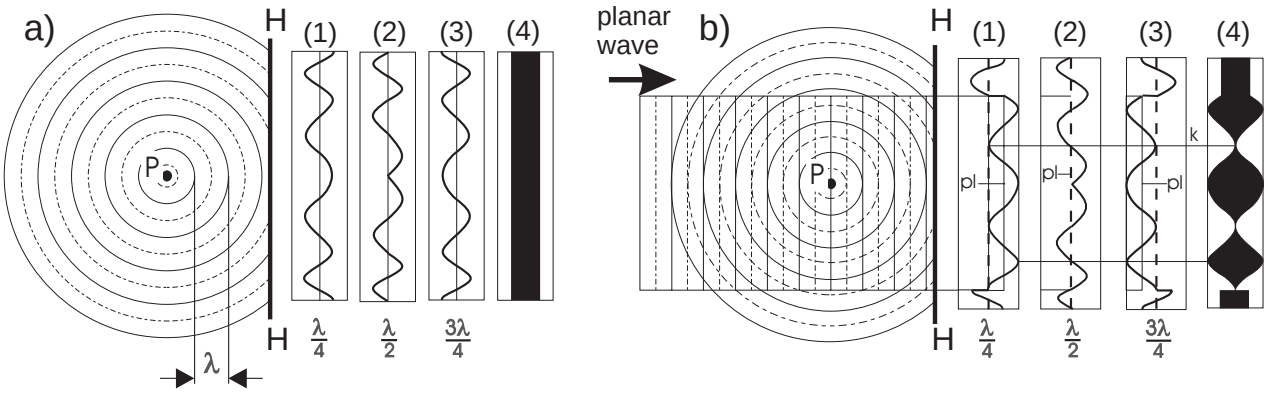

FIGURE 2: PRINCIPLE OF RECORDING A HOLOGRAPHIC-PLATE: A) WITHOUT A REFERENCE WAVE THE WHOLE PLATE IS ILLUMINATED WITH THE SAME INTENSITY, B) THE SUPERPOSITION OF THE WAVE COMING FROM POINT P (OBJECT WAVE) WITH A REFERENCE WAVE, THE PHASE OF THE INTERFERENCE-MINIMA IS CONSTANT BY TIME. PL = PLANAR REFERENCE WAVE, K = INTERFERENCE-MINIMA.

spherical wave coming from an object point P (= object wave- shown as circles in figure 2) would only darken a film in the hologram-plane (figure 2a (4)). This is caused by the permanent changing of the phase distribution of the light in the hologram-plane (figure 2a (1), (2), (3) with a phase difference of •/4 each.

By superposing a coherent reference (in this case a planar wave, with the same wavelength as the object wave) a constant distribution of the interference-minima by time (figure 2b) is produced. This is caused by the same velocity both waves pass the holographic-plane, and so the relation between the phases keeps the same. On the film microinterference-lines are created[1], which lead to a hologram after developing a plate which can be illuminated in this holographic plane.

This hologram is now a tool, to reconstruct the original waveform. In figure 3, recording and reconstruction of an off-axis[2] hologram is shown. By illuminating a hologram with the reference wave again, the ringsystem on the photographic emulsion works like a diffraction grating, with a decreasing of the grating constant by increasing diameter. Because of the diffraction of the reference wave at this grating, one zero-order wave plus two first-order waves appear. One of these first-order waves travels in the same direction as the original object wave and has the same amplitude and phase distribution. This spherical wave corresponds to the recorded object wave and creates the virtual image P'. The second first-order wave goes to the opposite direction and creates a real image of the object behind the photographic plate. This real image can be studied with various reconstruction devices, like a microscope.

To create a hologram of a complex object, this object has to be illuminated by a monochromatic light source. The reflected, scattered light (object wave) has obviously a very complicated waveform. According to the principles of Huygens, one however can regard it to be the superposition of many elementary spherical waves. The microscopic pattern of the hologram (which consists of up to 3000 lines/mm) contains now all information (amplitude and phase) about the complete wave.

Holograms have some interesting characteristics:

• As the reference wave, which is coming from one object point P covers the whole hologram, also in a small part of the hologram the total information of the object is recorded. Observing a part of the hologram, one just has to come closer like looking through a window.

• By changing the view angle, also the perspective changes as different reconstructed waves reach the eye.

• On a hologram a couple of exposures can be made, without changing the position of the plate. By reconstructing the hologram a superposition of the images takes place. This can be used either for a double-pulse technique to determine velocity-fields or for holographic interferometry (Mayinger, 1994). By this method, the first image of the measurement chamber in reference conditions is taken and the second image is a recording of the same measurement chamber with a variation of the temperature or density field. These two special application will be described below. For conventional application of holography lasers, emitting continuous monochromatic light, can be used. The recording of very fast moving or changing objects needs ultra-short exposure times, which can be achieved by a pulsed laser. A holographic set-up, using a pulsed laser is shown in figure 4.

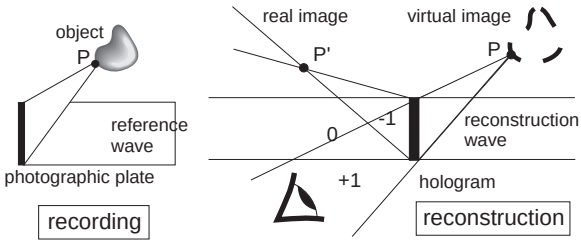

FIGURE 3: RECORDING AND RECONSTRUCTION OF AN OFF-AXIS HOLOGRAM. THE MICROSCOPIC PATTERN ON THE HOLOGRAPHIC PLATE ACTS LIKE A DIFFRACTION GRATING WITH A LOCAL VARIABLE GRATING CONSTANT.

[1] In this case of the superposition of a spherical wave with a planar wave, a system of circles, with decreasing distances by increasing diameter is created, called "Fresnel-zone-system".

[2] In an "off-axis" holographic set-up, the objective wave and the reference wave come from different direction, in an "in-line" set-up the objective wave concides with the reference wave, like shown in figure 2.

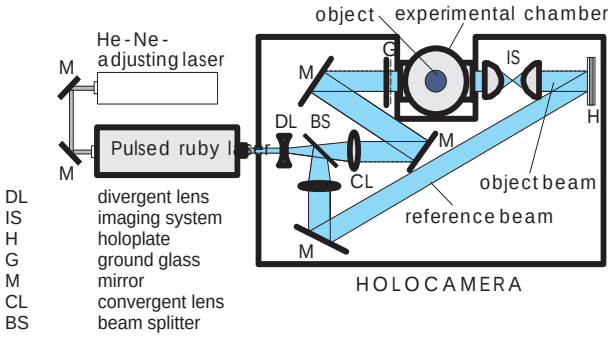

FIGURE 4: HOLOGRAPHIC SET-UP FOR ULTRA-SHORT TIME EXPOSURES WITH A PULSED LASER. AS THE PULS DURATION OF A RUBY LASER IS ABOUT 30ns, A CONTINUOUS LIGHT EMITTING HE-NE-LASER HAS TO BE USED FOR THE OPTICAL ADJUSTMENT.

In this arrangement, the light, emitted by a pulsed ruby laser (wavelength • = 693 nm, pulse duration 30 ns) travels through a system of a beam splitter, lenses and mirrors, where it is expanded, divided and guided through the measuring object onto the holographic plate. This set-up is suitable for studying particle flow or phase distribution in multiphase mixtures. It allows to visualize dispersed flow – like in post dry-out heat transfer with droplets not smaller than 10 times the wavelength of the laser light.

For evaluating the hologram it first has to be reconstructed, as demonstrated in figure 3. After the chemical processing the holographic plate is illuminated by a continuously light emitting helium-neon laser. If the holographic plate is replaced in the same orientation as during the recording process, a virtual image of the droplet cloud can be seen exactly at the place where it was produced previously. For a quantitative evaluation an enlarging lens or a microscope can be connected to a camera. To do this, the holographic plate has to be turned by 180°, so that the real image, which has a three-dimensional extension, appears in front of the camera. With a macroscopic lens, only a very narrow area of the spray will be well focused and by moving the camera forwards or backwards, the image can be evaluated plane by plane. The decision about the sharpness of a contour is made by a digital image processing system described in detail by Chavez and Mayinger, 1992 and Mayinger, 1996. An example of the result of such an computer-aided image processing is shown in figure 5. The upper row in this figure shows the region of the spray near the nozzle, and the lower one, a region further downstream, where the veil is already disintegrated into a droplet swarm. By applying specially developed algorithms (Chavez, 1991), the cross-section area, the diameter and the concentration of the droplets can be determined automatically.

This figure (5) gives an impression how the numerical procedure changes the original photographic picture into a computerized one, which contains only information of particles, being exactly in the focus plane, a slice, which is thinner than 0.5 mm in this case. The first module of the software transforms the original image (A), seen by the videocamera into a binary image. This original image of a holographic reconstruction is smoothed (B) and treated with a gradient filter (C). Sharply imaged structures are detected, edged and filled. Finally the image is binarized (D). An additional tool in this module allows to analyse either the big structures like the liquid veil (E, above) or only the smaller structures like droplets (E, below).

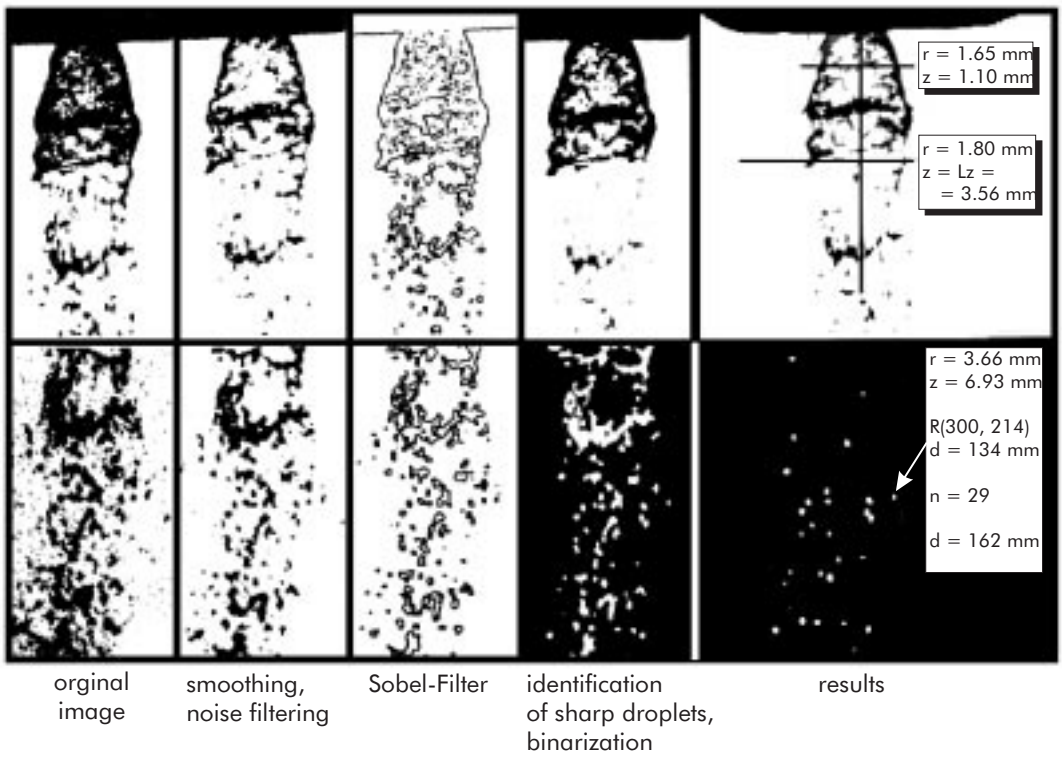

FIGURE 5: STEPS OF IMAGE-PROCESSING OF A HOLOGRAM

Double-pulse holography. As mentioned above, it is possible to illuminate the photographic emulsion of a holographic plate sveral times before processing. For example, this can be done with a ruby laser, which allows to emit more than one laser pulse within a short period of time (1 - 800 •s). With this method the velocity of droplets as well as their changes in size and geometric form can be evaluated (Chavez and Mayinger, 1992). The method of velocity measurements becomes complicated, if the motion of the particles is strongly three-dimensional. In such a case, pictures of a series of focus planes have to be scanned, digitized and correlated to each other to find the same droplets, which were exposed at different times and are located in different focal planes. A computer code using a Fourier analysis to do the evaluation algorithms can be found in literature (Gebhard, Mayinger, 1996).

Nevertheless, this technique becomes more and more difficult when the droplets of the spray have different direction as usually within technical applications of sprays. Hence a new method called ”stereomatching” was developed, where two holograms are recorded simultaneously, perpendicular to each other. The optical set-up in shown in figure 6, for the evaluation, both holograms have to be scanned and digitized by a camera, which is still focused stepwise along the depth co-ordinate in order to record the entire 3-D information contained in the holographic image. For the handling of this huge amount of data, the software described above was extended for the stereomatching, which is described by Feldmann, et al., 1997.

Holographic Interferometry

Up to the 70th mostly the Mach-Zehnder-interfermometry was used for optical investigation of temperature fields, temperature gradients and heat transfer coefficients. A planar light wave, coming from the left side is divided into two object waves by a semipermeable mirror. The first object wave passes through the test section, while the second object wave is going the way around the test section. Caused by a temperature or density gradient in the test section, the phase distribution of the first object wave changes. The two waves are superposed after another semiper-meable mirror. This leads to a macroscopic interference, which shows the temperature or density field in the test section. This macroscopic inter-ference caused by a temperature gradient must not be mixed up with the microscopic interference, we use for holography (as mentioned in chapter 2).

The optical set-up for this technique has to be very precise and all optical devices have to be best quality, as a small difference of the refraction index on the way of the two light waves leads to an unintentional interference. In the case of a closed test section with windows, two equal ones, have to be applied, to ensure two equal beam paths.

The holographic Interferometer avoids these problems of Mach-Zehnder-Interferometrie, as for the second object wave the holographic reconstruction of the test section is used. Thus two waves are superimposed, which pass through the same test section at different moments, and changes, which occur between the two recordings are interferometrically measured. To determine for example the heat transfer, the recording of the first wave is made, when all desired processes in the test section are in operation (fluid flow, pressure and mean temperature) but not that process (the heat transfer from a plate or from a bubble) which is of interest.

In the following, two techniques doing this are explained:

- double exposure technique and
- real time technique.

As described before several object waves can be recorded, one after another, on one single holographic plate before the photographic emulsion is being developed. By illuminating the plate with the reference wave, they are all simultaneously reconstructed (figure 7). If they differ slightly from one another, the interference between them can be observed (figure 7, lower part). In this example the first recording was done, when the test section (tube) had a constant temperature distribution. After that a temperature field was established by heating up the wall of the tube. Now the incoming light waves received a continuous, additional phase shift, due to the temperature field. This wave front (measuring beam) was recorded on the same plate. After processing and illuminating the hologram, both waves were reconstructed simultaneously and they interfered.

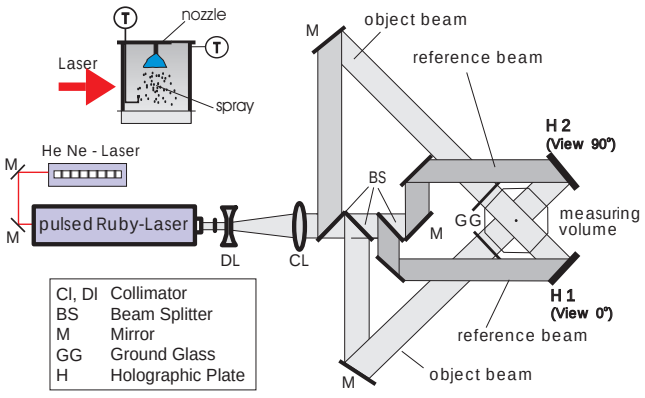

FIGURE 6: HOLOGRAPHIC SET-UP FOR STEREOMATCHING OF STRONGLY THREE-DIMENSIONAL MEASUREMENT PROBLEMS. THE TWO HOLOGRAPHIC PLATES ARE EXPOSED AT THE SAME TIME.

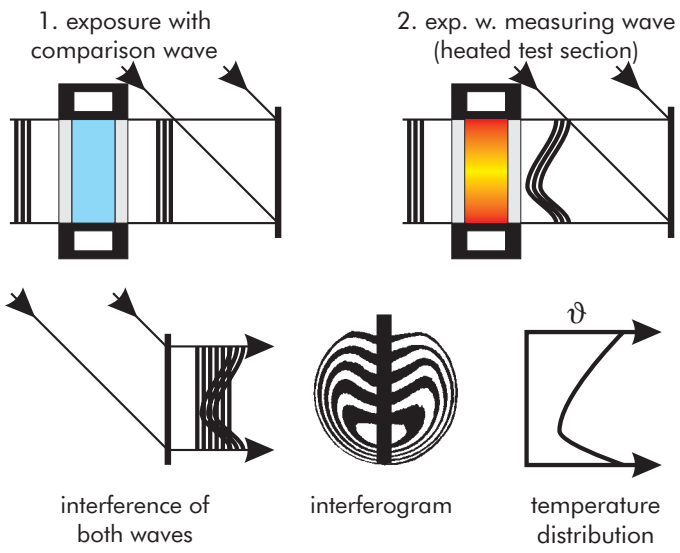

FIGURE 7: PRINCIPLE OF THE DOUBLE EXPOSURE TECHNIQUE

By this method – in comparison to conventional interferometry techniques – the same object beam is compared at different times. Since both waves pass through the same test section, any imperfections of the windows, mirrors and lenses are eliminated. Examinations even at very high pressures can be made, because the deformation of the windows can be compensated.

This method of double-exposure technique is simple to handle, however, the investigated process cannot be continuously recorded and the result of the test can only be seen after developing the photographic emulsion.

Infinite fringe method (real time). To overcome this problem a more sophisticated recording process for holographic interferometry, the real-time method, was developed, illustrated in figure 8. After the first exposition of the hologram, during reference conditions of the test chamber, the hologram is photographically developed and fixed. The plate is exactly repositioned to the former place in the optical set-up. This can be done with piezo quarz positioning devices with an accuracy of half a wavelength. By illuminating the hologram the comparison wave can be reconstructed continuously. This wave can now be superimposed to the momentary object wave. If the conditions in the test section are not changed, compared to the situation of the first exposure, no interference fringes will be seen on the hologram ("infinite fringe method"). This indicator can be used for replacing the hologram exactly to its old place. By starting the heat transfer process, the object wave receives a phase shift, due to the temperature field in the examined fluid. Both waves interfere with each other, and the changes of pattern can be continuously observed or filmed.

In figure 9 an example of detachment and recondensation of bubbles from a heated wall is shown. The black and white lines – called fringes – in these interferograms represent in a first approximation isotherms in the liquid. So if the fringes are close together, there is a steep temperature gradient, fringes far apart from each other show a plateaux of almost constant temperature. One limitation of this optical measurement method can also be seen in figure 10. Of course, the light passing the test section is not only shifted in phase. It is also deflected, depending on a positive or negative temperature gradient, to the wall or from the wall. Hence a thin zone very near to the wall appears as a grey pattern without interference fringes.

Evaluation of the Interferograms. As described before, the physical principles of the interference effect of the holographic interferometry are similar to Mach-Zehnder interferometry. The difference of both methods is the origin of the reference beam, which has no influence to the interference effect due to a temperature field in the test section. Thus the evaluation of both methods is quite similar to each other and can be found in literature (Mayinger and Panknin 1974, Mayinger 1994). However, to obtain absolute values for the temperature field, the temperature at one point of the cross section has to be determined, for example by thermocouple measurements. This is usually done in an undisturbed region or at the wall of the test chamber.

All examples of measurements discussed by now are of two dimensional nature, but also three-dimensional temperature fields, for example, spherical and cylindrical temperature fields, can by measured by holographic interferometry. In this cases, the Abel correction has to be used, which is described by Hauf and Grigull, 1970 or by Chen, 1985.

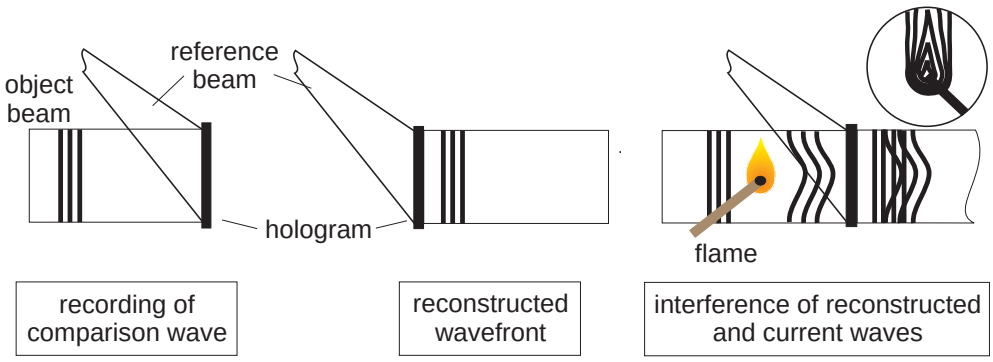

FIGURE 8: PRINCIPLE OF THE REAL TIME METHOD

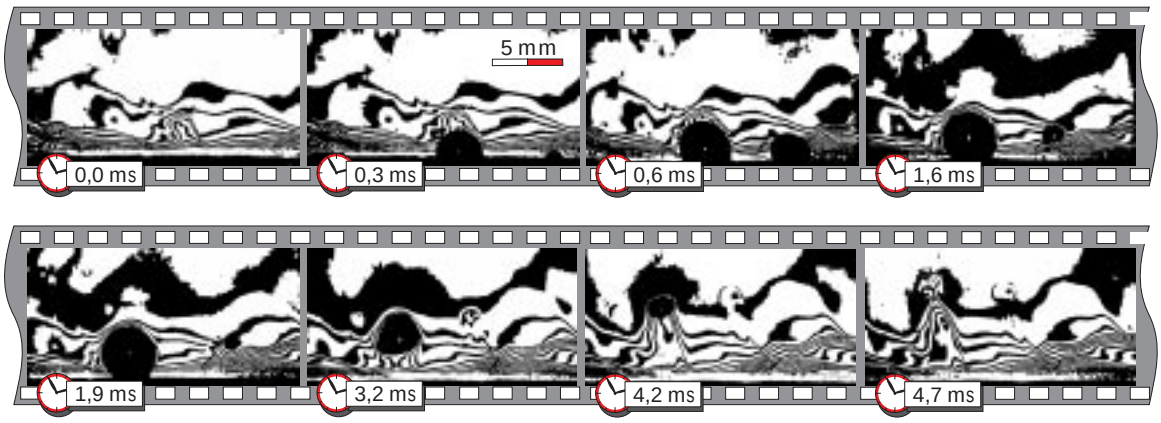

FIGURE 9: DETACHMENT AND RECONDENSATION OF BUBBLES FROM A HEATED WALL

Finite Fringe Method. As the boundary layer at a heat-transferring surface becomes very thin, with higher heat transfer coefficients, it is quite difficult to evaluate the interference pattern. In such a case it can be helpful, to create a pattern of parallel interference fringes after producing the reference hologram. This can be done by tilting the mirror in the reference wave of figure 8 or by moving the holographic plate within a distance of few wavelengths. The direction and distance of the "artificial" generated fringe pattern depends only on the direction of movement of the holographic plate or mirror. The result of the so called ”finite fringe method” is compared to the earlier described ”infinite fringe method” in figure 10. By imposing a temperature field, due to the heat transfer process, the parallel fringes are deflected, which is a measure for the temperature gradient. This allows to deduce the heat flux and by this the heat transfer coefficient. The detailed evaluation process is described well in Chen et al. 1991.

Two-wavelength method. The light passing the measurement volume cannot only be phase-shifted by a temperature field but also by locally different densities, caused by concentration gradients. In these cases two unknown variables – temperature and concentration - have to be found, by solving the interferometric equations. This can be done by using two laser simultaneously, emitting light of two different wavelengths. As the refractive index is depending on the wavelength of the light (as known from the rainbow phenomena), two sets of equations are available – one for each wavelength – and the system is solvable for two unknown variables. The problem of this method, described in detail by Panknin and Mayinger (1978), is, that the two interferograms originating from these two beams of different wavelengths have to be superimposed very accurately. As already described, it is possible to record different interference pattern on one and the same holographic plate, which is done with the two-wavelength method.

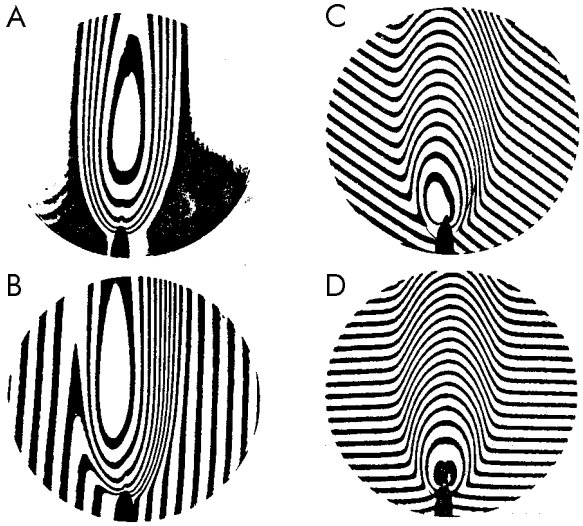

FIGURE 10: INFINITE FRINGE METHOD (PICTURE A) AND FINITE FRINGE METHOD WITH DIFFERENT ORIENTATIONS OF THE UNDISTURBED FRINGES: B: VERTICAL, C:INCLINED, D: HORIZIONTAL

Light Scattering Methods

The lower part of table 1 shows some of the most common light scattering techniques, used for thermo-fluiddynamic investigations. A summarisation and detailed explanation of various light scattering methods can be found in Eckbreth 1988.

These methods are based on the principle that photons are in interaction with particles, which are lifted to a higher rotational, vibrational or electronic level. After a certain time - depending on the special technique - the particle drops back (but not always exactly to the same level as before) and emits light of a special wavelength. To get a high light flux and a well defined wavelength of the incoming light, mostly laser are used as light sources.

Scattering processes having the same wavelength as the exciting light wave are termed elastic processes, if a shift of the wavelength occurs, the phenomena is termed inelastic scattering process.

Mie scattering. The elastic scattering process, where the size of the scattering particle is bigger or not much smaller than the wavelength of the incoming light is called Mie scattering, which is a very strong process. Unfortunately it is not dependent on the density, temperature or species concentration and hence cannot be used for the measurement of these dimensions. But this type of scattering can be used for some other very important techniques like particle image velocimetry (PIV), particle tracking velocimetry (PTV) or laser Doppler velocimetry (LDV).

PIV is a two dimensional method, where a laser beam is formed into a thin light-sheet illuminating a plane within the volume of

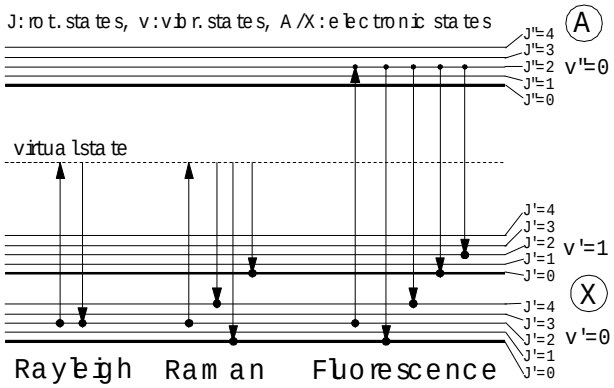

FIGURE 11: ENERGY DIAGRAMS

interest. Certain particles which have a density close to fluid are added to the flow. The radiation scattered by the particles in the illuminated area is recorded by a camera (with a very short exposure time) two times within a defined time spacing.

PTV is very similiar to PIV, but with the difference that there is only one exposure and that the exposure time of the camera is much longer. Thus trajectories of the particles can be observed which are correlated to streamlines of the flow.

With LDV (Durst, 1987) two laser-beams of the same origin are focused to a small measurement volume. When a particle passes this measurement volume, the Doppler frequencies of the Mie-scattered light can be directly transformed to velocities. With three different coloured pairs of laser beams, all three velocity dimensions can be determined simultaneously. As the datarate,

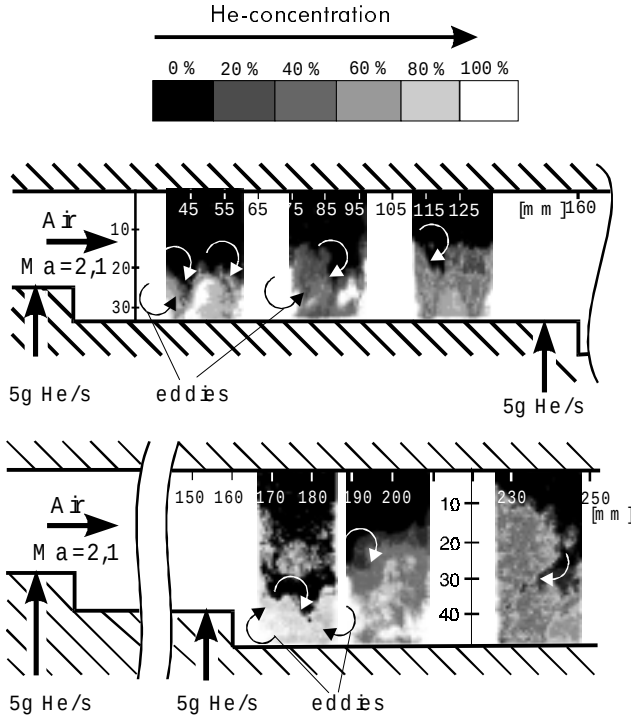

FIGURE 12: HELIUM DISTRIBUTION IN A SUPERSONIC FLOW, MEASURED BY RAYLEIGH SCATTERING

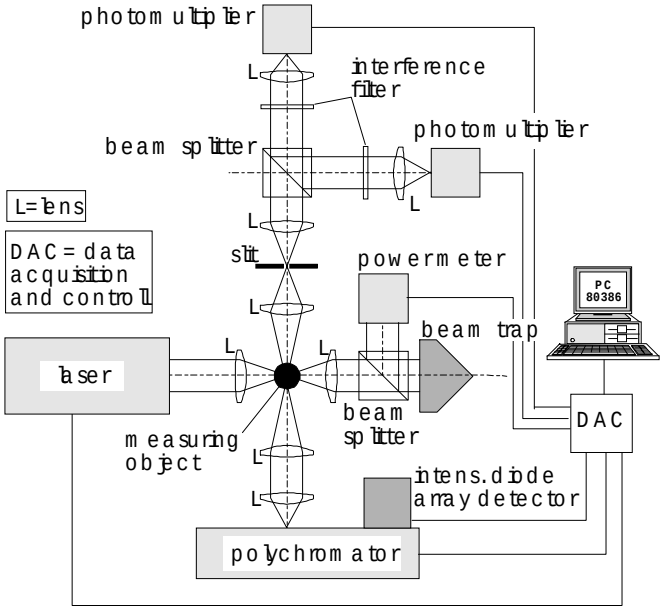

FIGURE 13: TYPICAL RAMAN SET-UP WITH TWO ALTERNATIVE DETECTION SYSTEMS. USUALLY ONLY ONE OF THE SHOWN POSSIBILITIES IS USED.

depending on the particles in the flow, is very high this method can be used very well to determine turbulence parameters.

Scattering processes of light quanta from molecules or small particles (with a diameter much smaller than the wavelength of the incoming light like molecules) are for example Rayleigh scattering, Raman scattering or Fluorescence (figure 11).

Rayleigh scattering. Rayleigh scattering can be observed, if after the interaction with incident light quanta the molecules return to the same state they were in previously. As it is an elastic process, the scattered photons have the same frequency as the incoming light, hence, the scattered signal is not specific to the species in the measurement volume. Therefore this method can be used to measure densities, and by using the gas law in constant pressure situations, also temperatures can be determined. Using a two dimensional optical set-up, this can be compared basically to the one used for laser induced fluorescence as shown in figure 15, keeping in mind, that different lasers, lenses and camera systems might be used. A laser is formed into a thin light-sheet by two lenses, and the Rayleigh scattered light is recorded perpendicular by a CCD-camera. One can imagine, that having particles in the test region leads to an additional Mie scattering process which cannot clearly be distinguished from Rayleigh scattering. So the experiments, examined with this method have to be of a clear, fundamental nature like the example shown in figure 12, where helium is added from two positions at the wall into a supersonic flowfield. These experiments were made to investigate the mixing processes in supersonic flows for future aircraft propulsions, in this case a scramjet, with hydrogen as fuel.

Raman scattering. The principle of Raman scattering as an example of an inelastic scattering process is shown in figure 11 b). By exciting a molecule with a photon, it is shifted to a non stable virtual state, from which it drops back within a time of 10^{-12} sec or less. But contrary to Rayleigh scattering, the molecule turns into a higher or lover level than the original one. Therefore

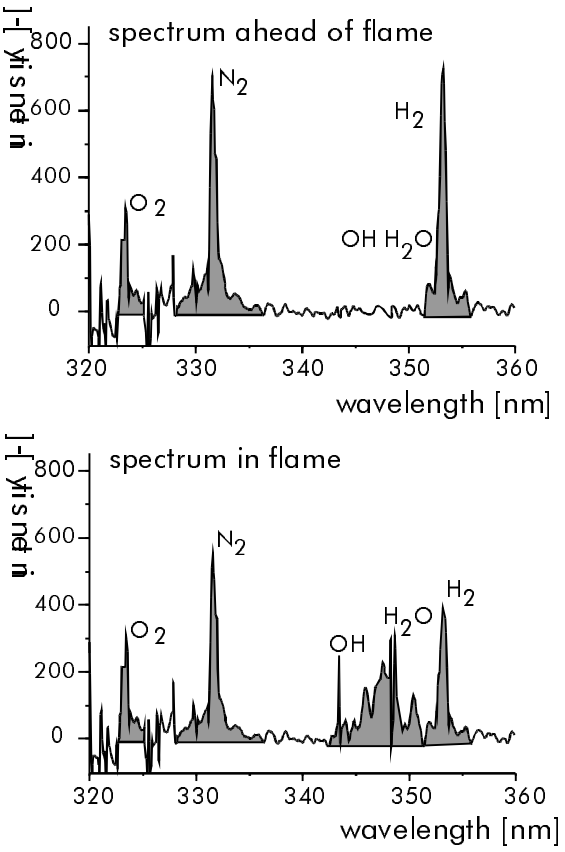

FIGURE 14: TYPICAL SPECTRA FROM A POINT IN A BURNER. A, UNBURNED MIXTURE WITH 12 % H_2 IN AIR. B, SPECTRUM FROM THE TURBULENT REACTION ZONE.

the scattered radiation is shifted from the incident light wave by the characteristic frequencies of the media. For historical reasons, a downshift in frequency is called Stokes, an upshift is called anti-Stokes. The fact, that the Raman scattered signal is species specific and linearly proportional to the number of species makes it a very useful tool for the examination of species concentration in combustion processes. Figure 14 shows an example of Raman scattering in a burner before and in an hydrogen-air flame (Mayinger et al., 1993). As the concentration of nitrogen can be assumed as being mainly constant, the different scattering intensities of nitrogen in this example can be used to determine the local temperature.

So far, Raman seems to be a perfect tool for the examination of concentrations and temperatures. Unfortunately, for practical use, Raman spectroscopy has also a couple of disadvantages compared to other scattering methods described here. The optical set-up is quite complicated, as the emitted light has to be spectrally analysed to identify the single species. By using a spectrometer as shown in the lower part of the optical set-up in figure 13 point or one-dimensional spectral analysis can be realized. Interference filters (shown in the upper part of figure 13) allow the observation of only one species per filter. However, the collected Raman signal to laser energy ratio in flames is about 10^{-14}, which leads to a very poor signal (even by using high energy lasers and specially intensified cameras) and bad signal to noise ratios.

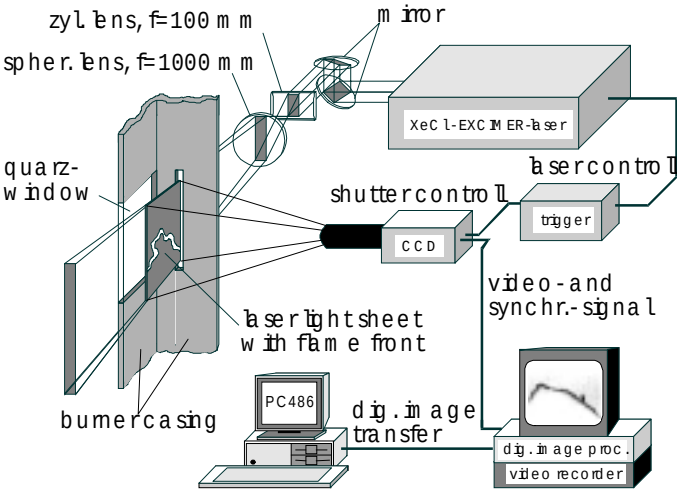

FIGURE 15: OPTICAL SET-UP FOR LASER INDUCED FLUORESCENCE

Laser induced fluorescence (LIF, LIPF). By choosing a laser wavelength, which allows to lift the molecule even to a higher electronic energy state the so called laser induced fluorescence can be observed (figure 11c) when the molecule drops back to a lower level again. As the level the molecule is lifted to is not a virtual state - as used with Rayleigh or Raman scattering - but a semi-stable state, the lifetime of the molecule in this excited state can be much longer (10^{-10} to 10^{-5} s). The fact that the laser induced fluorescence is species specific and the intensity of the scattered light is many orders of magnitudes stronger than those for Raman, makes it a very important tool for flame diagnostics.

However, radiation is not the only possibility for an excited

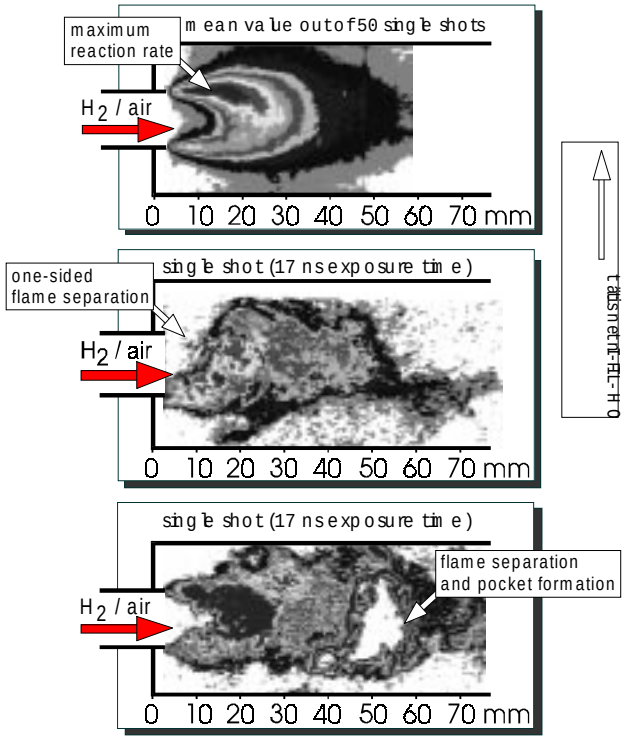

FIGURE 16: LIF AT A H_2-AIR DIFFUSION FLAME

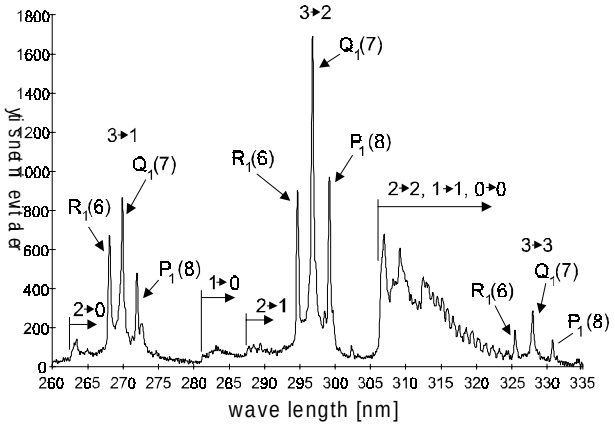

FIGURE 17a: SPECTRUM OF THE EMISSION OF OH EXCITATION WITH AN KrF-EXCIMER LASER (248,15 nm)

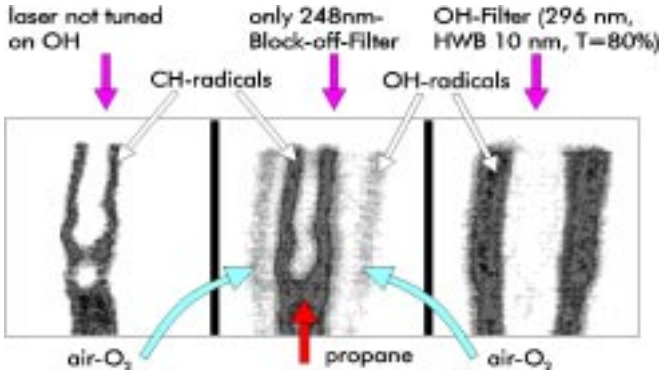

FIGURE 17b: OH-/CH-LIPF AT A C_3H_6 DIFFUSION FLAME

molecule to loose energy. Also dissociation, energy transfer to another molecule, energy transfer to other internal energy states within the same molecule and chemical reaction can take place and can summarised termed quenching effects. One can imagine that the main problem of these quenching effects is not only that they reduce the amount of fluorescence, but mainly that an quantitative interpretation of the observed fluorescence is nearly impossible, as the quenching rates are hardly ever known. However an analytical correction as far as possible can be found in literature (Eckbreth, 1988, Andresen, 1990, 1992), and there are several special techniques where there is no need for quenching corrections like the laser induced predissociation fluorescence.

The optical set-up can be simplified like drawn in figure 15. As described before, a thin laser light-sheet is formed by two lenses and a camera with a special lens and filter is recording perpendicular one or more fluorescence lines of one single species.

Figure 17a shows an example spectrum of laser induced fluorescence. The excitation of the OH-radicals can be realised by using a pulsed excimer laser run with XCl, which has a wavelength of 308 nm, and an extremely short pulse duration of 17 ns. Two of these very short shots of a flame in a burner are shown in the lower pictures of figure 16. In the picture in the middle, the flame is separating from the injection spot of the burner, in the lower picture a non reacting zone – in spite of a homogeneous mixture of fuel and air – can be observed over a long flowpath of the flame.

By using this method, one has to be aware of the fact that the laser induced fluorescence as used in such a manner with an excitation wavelength of 308 nm for OH is an elastic scattering process, thus the scattered signal can be interfered by Mie scattering of particles or reflection at windows or walls.

One possibility to get quantitative species concentration out of an fluorescence signal is the so called laser induced predissociation fluorescence (LIPF). Hereby a state with a very high dissociation rate is excited with light of a special wavelength. This dissociation happens that fast, that the other quenching effects mentioned above can be neglected. To excite the OH-radical in that way a KrF-excimer laser (wavelength • = 248 nm) can be used. As this transition dissociates strongly, the scattered fluorescence signal is much lower than using LIF with 308 nm, but the signal can be quantified much easier. For practical use, due to the relative low signal, the experiment has to be as clean as possible. The test chamber should be free of reflection (as with all light scattering processes), and due to the fact that ordinary glass is not transparent for light of 248 nm (as well as for 308 nm) the windows have to be made out of quartz glass. Using this wavelength for excitation, the fluorescence signal appears frequency shifted with a wavelength of 295 – 304 nm as shown in figure 17a. Using a filter, interfering signals can be almost tuned out. In figure 17b a propane diffusion flame is shown to demonstrate the effects of laser tuning and block-off filters.

To demonstrate the capability of this optical method, the influence of the hydrogen concentration on the flame structure in an unsteady smooth tube burner is shown (figure 18). At low hydrogen concentration, the single flamelets are not able to work against the buoyancy in the tube, so the flame is locally quenched. With 12% hydrogen in air, this effect is not that strong anymore, but still quenched zones can be determined at the negative curved areas of the flame. Adding more hydrogen (16%), a pocket separation at the flamefront takes place, which leads to bigger surface of the flame and to higher flame velocity.

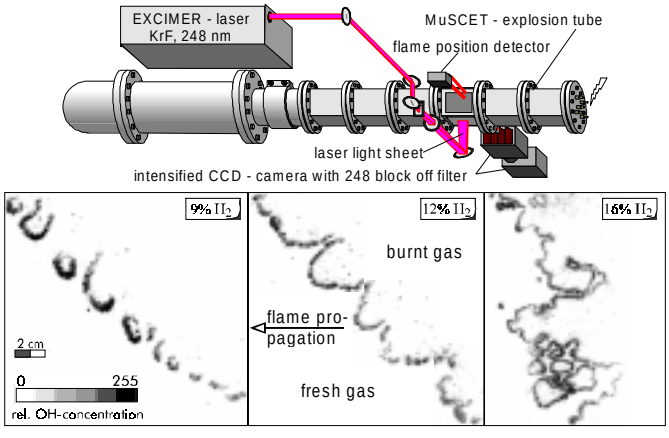

FIGURE 18: LIPF IMAGES OF HYDROGEN AIR FLAMES IN AN INSTATIONARY TUBE BURNER

Classical Optical Measurement Methods Combined with New Camera Devices

The camera equipment which is on the market nowadays opens new opportunities for classical measurement techniques like the Toepler-Schlieren method or even the oldest known measurement technique, the examination of the so called self-fluorescence, which appears with reacting gas-mixtures undergoing high enthalpy differences, and can be observed even with the naked eye. It is based on the fact, that during a chemical reaction some of the particles already arise in an electronically excited state. A part of these excited particles radiate energy by spontaneous emission of photons in connection with a change in the energetic state of the molecule, which is refered to as chemo-luminiscence. In figure 19 an example of the burning process in a ship engine driven with hydrogen is shown, where self-fluorescence occurs mainly during the OH-production.

Years ago, drum cameras - using photographic film material - were used to produce such high speed photographs. Depending on the spatial resolution repetition-rates of some 10.000 images/sec could be realised, by using a pulsed light source like a flash lamp. One of the main disadvantages of this method was the handling of the photographic material. Due to the whole film developing process, the result of an experiment could be seen only half an hour after the experiment itself.

With modern high speed videocameras, it is possible to record sequences with repetition-rates of 45.000 images/sec and to store several thousand images in the internal memory of the system online. Immediately after the experiment, the result can be seen as a video film. Storing images in the computer for further processing works mainly automatically and is done within a few seconds per image. Another big advantage of this new high speed videotechnique is, that the internal image memory of the system can be overwritten continuously. By setting a trigger signal the camera stops recording and the last for example 1000 images taken before the trigger signal are kept in the memory. It is also possible to set the trigger signal in the middle of the experiment and to keep 500 images before and 500 images after the trigger. By investigating self-igniting combustion processes this is a very helpful tool, as the ignition time can not always be predicted precisely. Nevertheless the resolution of such a video system is 512 times 512 pixels, which is only a very small part of the resolution of classical photography.

With such a high speed video camera system the schlieren method developed by Toepler 1864 can be used in a new way for highly transient processes like the combustion in a closed tube. The combination of an old but very sophisticated optical measurement technique with newest recording devices gives a very good insight into the dynamic processes of flame acceleration by obstacles as horizontal tubes, plates and wall-openings (figure 20). The principles of the schlieren-technique itself, the optical set-up and the evaluation of the data can be found in literature (Hauf et al. 1991).

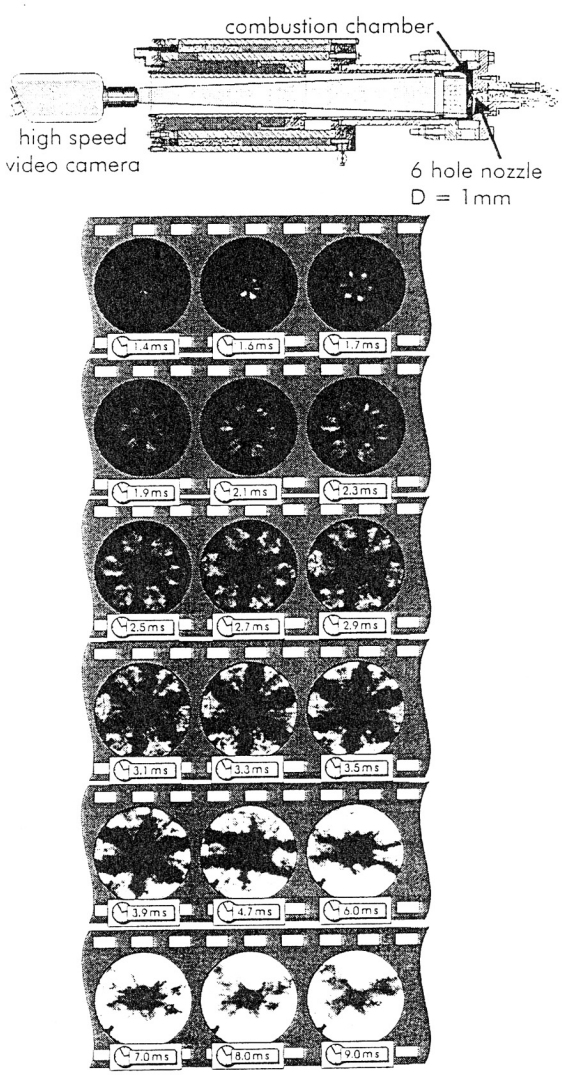

FIGURE 19: SELF-FLUORESCENCE IN A SINGLE-STROKE ENGINE WITH A PISTON DIAMETER OF 250 MM

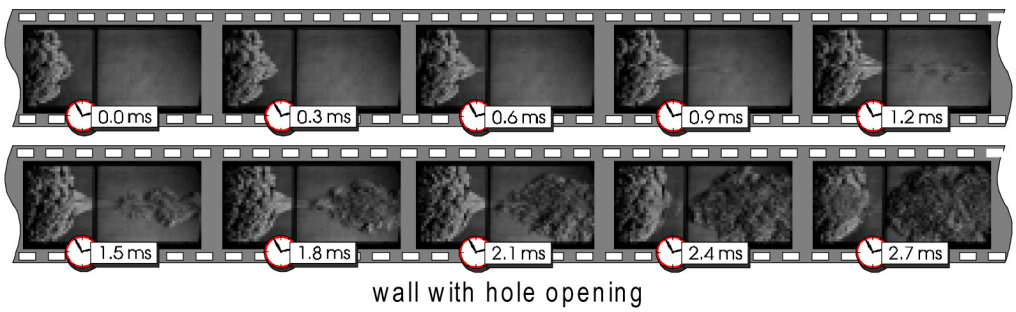

FIGURE 20: HIGH SPEED VIDEO SCHLIEREN TECHNIQUE, SHOWING THE FLAME ACCELERATION BY OBSTACLES DURING THE COMBUSTION PROCESS OF H_2 IN AIR IN A CLOSED TUBE (WALL WITH HOLE OPENING)

INVESTIGATION OF HEAT TRANSFER BY OPTICAL TECHNIQUES

Plate Heat Exchanger with Rib-roughened Surfaces

Forced convective heat transfer in channels with rectangular cross section was investigated (Re_{max} = 7.000). To enhance the heat transfer, rib-roughened surfaces are applied to the wider walls of the duct. Various rib shapes, rib spacings and rib arrangements have been investigated. Temperature fields, velocity fields and the distribution of turbulent kinetic energy within the duct were obtained by holographic interferometry and laser Doppler anemometry.

The test section (figure 21) consists of a rectangular duct with isothermically heated upper and lower aluminium walls. The side walls are made of glass to allow optical access. The test section is connected to a smooth 700 mm inlet duct (adiabatic) and a 150 mm outlet duct with the same aspect ratio. The unheated inlet section leads to an almost hydrodynamically developed flow, with a thermally developing flow regime in the heated test section. The upper and lower test-section walls have rib-roughened surfaces. Ambient air is sucked into the inlet section of the heat exchanger by a compressor equipped with a flow-regulating throttle. Volume flow rates in the channel are determined by the pressure drop at orifices, and verified by rotameters. Air temperatures at the entrance and at the exit of the test section are measured by thermocouples. Pressure drop in the test section is measured by an inclined tube manometer. The mean heat transfer rate in the duct was calculated from temperature and flow rate measurements of the air flow.

Figure 22 shows interferograms of the duct flow at different Reynolds numbers (Re = 500, 1500, 2500 and 5000) for a rib spacing of p/e=10; the fringes represent isothermal lines in the temperature field.

These interferograms show the size of the recirculation zones behind the ribs and the wall reattachment points of the flow. The effect of the ribs to induce turbulence can be seen especially in the interferograms for Re = 1500. While the flow is still laminar at the beginning of the test section, it becomes turbulent approximately in the middle and is fully turbulent at the end. Out of these interferograms, the local heat transfer can be calculated (figure 23) by measuring the distances of the isotherms along perpendicular lines to the heat transfering surface, as described above. It can be seen that the Nusselt number always has a maximum located almost at the top of a rib, a minimum just behind the ribs, and, depending on Reynolds number, a second local maximum in the spacing between the ribs. This is due to the fact that at a certain velocity, the flow separates at the rib top, and areas behind the ribs develop where the fluid is recirculating, causing poor heat transfer in this area. The local maxima in the Nusselt number in the spaces between the ribs result from reattaching flow. Higher flow

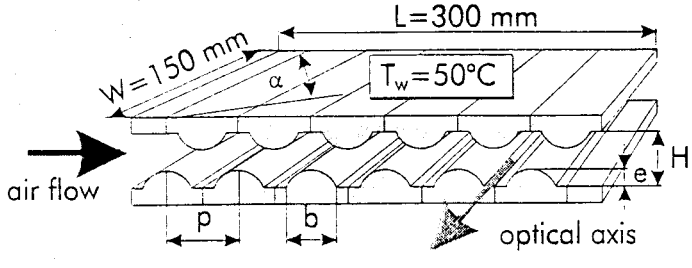

FIGURE 21: TEST SECTION

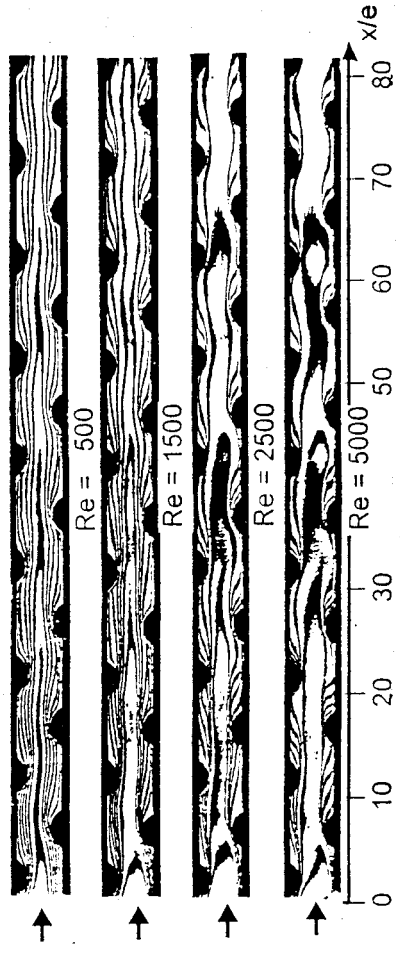

FIGURE 22: INTERFEROGRAMS OF DUCT FLOW

velocities lead to an increase in the mean heat transfer. Figure 23 confirms that the increase results mainly from a better heat transfer between the ribs, while the heat transfer at the ribs itselfs increases only slightly. The turbulence-inducing effect of the ribs can also be determined by LDV measurements of the turbulence intensity of the flow (figure 24).

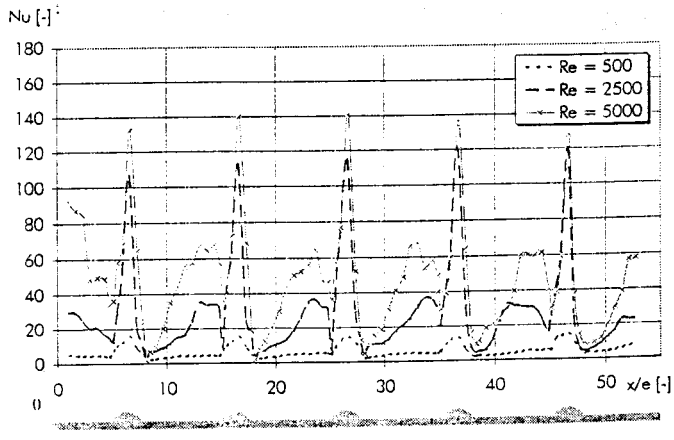

FIGURE 23: LOCAL NUSSELT NUMBER

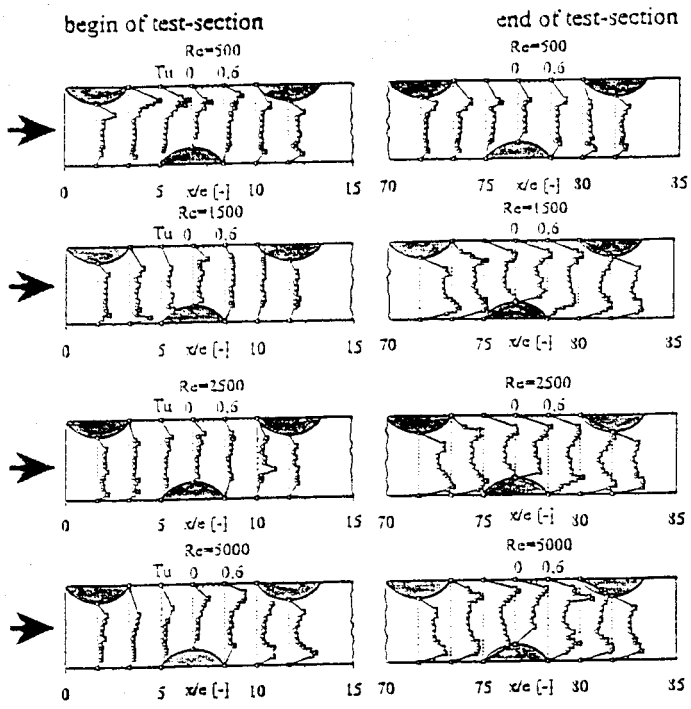

FIGURE 24: TURBULENCE INTENSITY

Different parameters like rib spacing, rib shape, rib angle and rib arrangement have been investigated. To judge the performance of the configurations the relation Nu/Nu_0 vs. $\xi/\xi_0^{1/3}$ (i.e. heat transfer vs. friction factor related to a smooth duct) was evaluated. With this criterion all the data refer to the same pumping power for the fluid. The influence of the rib spacing is presented in figure 25 (Tauscher and Mayinger, 1997).

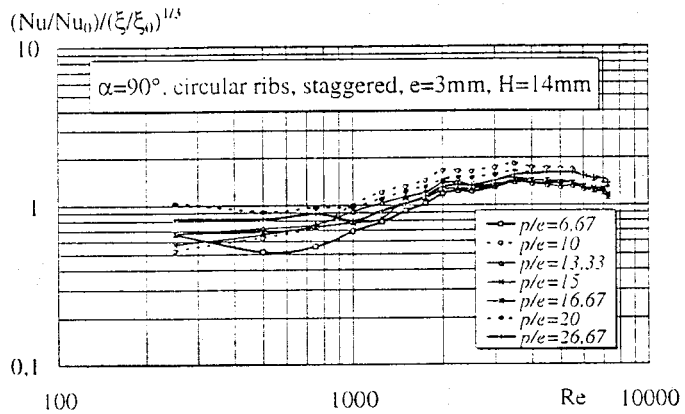

FIGURE 25: INFLUENCE OF RIB SPACING ON HEAT EXCHANGER PERFORMANCE

Enhancement of Forced Convection Cooling of Highly Loaded Heat Sources in a Rectangular Channel by Flow Deflection.

Efficient and effective cooling of electronical components is directly related to reliability and lifetime of the device. Cooling of high power chips challenges the thermal engineer because temperature limits become more constraining.

The object of the investigation presented below is to enhance the turbulent heat transfer from discrete heat sources in a rectangular channel with inclined plates positioned along the channel centerline. The periodic positioning of the plates accelerates the flow, enhances turbulence and reduces the thickness of the thermal boundary layer periodically at the heaters. With thin boundary layers higher heat transfer coefficients are associated because thermal resistance is reduced.

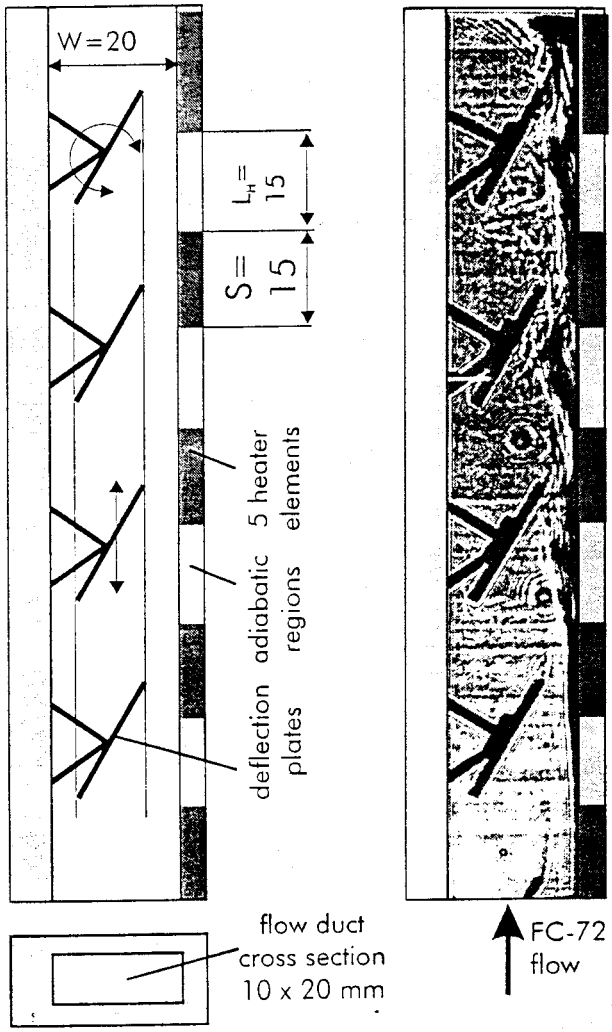

FIGURE 26: TEST SECTION AND SHADOWGRAPH OF FLOW

The experiments were performed in a rectangular duct with 5 heaters flush mounted in one narrow side of the vertically oriented channel. The heater length in flow direction is L_H = 15 mm, their width is H_H= 4 mm with an equal spacing of S = 15 mm to each other. The 5 defleciton plates were mounted on the opposite wall on a movable sledge so that the vertical position of the plates relative to the heaters could be variied. Three different sledges with plates positioned at inclination angles of α = 20°, 30° and 40° were used. It is important to mention that the plates are designed in such a way, that they have the same projected width i.e. blockage effect for any of the three inclination angles. So the distance between the edges of the plates and the short sides of the duct is 5 mm on both sides in any case (figure 26). Glass side walls allow

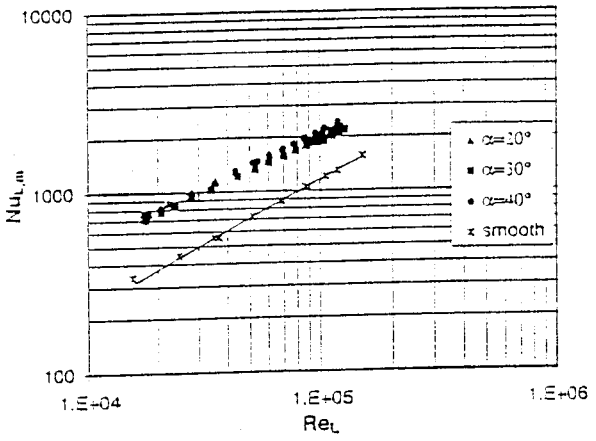

FIGURE 27: EFFECT OF PLATE INCLINATION ANGLE

optical access for measurements by LDV and the shadowgraph method.

The Reynolds number, based on the hydraulic diameter ranges from Re = $1.3x10^4$ to $1.5x10^5$. The improvement of heat transfer is attained by deflecting a stream of liquid (FC-72) directly to each heat source like a submerged jet by means of the inclined deflection plates. All of the experiments were conducted under conditions of equal and constant heat flux from each of the 5 heaters.

Effect of inclination angle. The experimental results presented in figure 27 show that the 20° and 40° inclined plates enhance the heat transfer more than the 30° configuration. On the other side the pressure losses were also higher for 20° and 40° than for the 30° which shows an analogy between momentum transfer and heat transfer. Different inclination causes a different impact of the plates as flow deflectors (jet effect) or turbulence promotors.This is confirmed by measurements of the flow velocity and turbulence intensity in the free cross section area at the heater side done by LDV. Considering pressure drop and heat transfer and relating the results in form of the flow area goodness factor, for example, the 30° configuration reaches the highest values. The effect of heater row, behavior of the first heater was investigated as well as the effect of the plate position. For detailed informations please refer to Fehle (1996).

Flow visualization and heat transfer optimization in a glass melt tub

The following example shows the application of a combination of particle image velocimetry (PIV) and particle tracking velocimetry (PTV) to get informations on the flow field in a glass melt tub and thus to optimize the heat transfer. The main process in the glass producing industries is the glass melt process itself. The melting process is responsible for the product quality and the power demand and still has a lot of of possibilities for optimizations. The quality of the raw glas is mainly dependend on a homogeneous matter and temperature of the glass melt in the tub. The glass flow in the melting tub is influenced by the geometry of the tub on one hand and on the other hand by the different kinds of

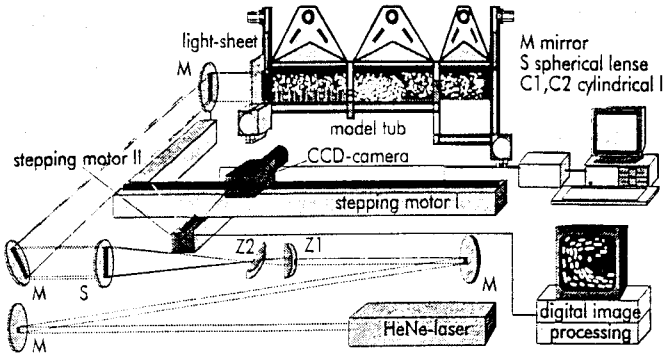

FIGURE 28: OPTICAL SET-UP

energy input and output mechanisms. The basic conditon for any optimization ist the knowledge about the flow field within the tub

The optical set-up of the experiment is demonstrated in figure 28. To visualize the velocity field particles of the same density as the fluid are added, their streamlines recorded with a CCD-camera and evaluated with a computer based image processing system. The illumination of the tub is done with a laser light sheet, which allows to capture well defined planes of the tub. Thus all other (non-illuminated) regions can be faded out. The camera as well as the light-sheet are shifted by stepping motors assuring, that whole the tub can be observed successively. The flow images recorded by the camera are filtered and evaluated by image processing algorithms. The result will be a two dimensional velocity field. The usage of a conventional PIV system often causes problems with the clear allocation of the same particle recorded at different times. These ambiguities can be avoided by a skilful combination of single images („PIV") with a pseudo long time exposure („PTV"), realised by image adddition. The frame grabber can store up to 12 images with a resolution of 512x512 pixels. One part of the memory is used to visualize the instantaneous image, another one to build a connected image done by an online image addition, which delivers (similiar to long time exposure) the trajectories of the tracer particles over the whole measuring time. The remaining ten memory regions are mapped with images of the instantaneous flow pattern at defined times but with a very short exposure time to get only small screen pixels from each particle. After filtering the images by special algorithms (noise filter, contour filter, etc.) the outlines of the pixels and the trajectories are taken and saved together with their coordinates. Besides the coordinates also the grayscale distribution is considered to find the center points, enabling the system to find the centers of gravity of the pixel areas, respectively the centerlines of gravity of the trajectory bands.

The calculation of the velocity vectors is always done by the evaluation of the local coordinates of the trace particle at defined times. The allocation of the tracer particle pixels recorded at

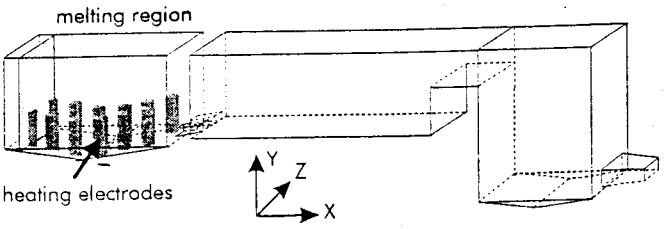

FIGURE 29: MODEL TUB

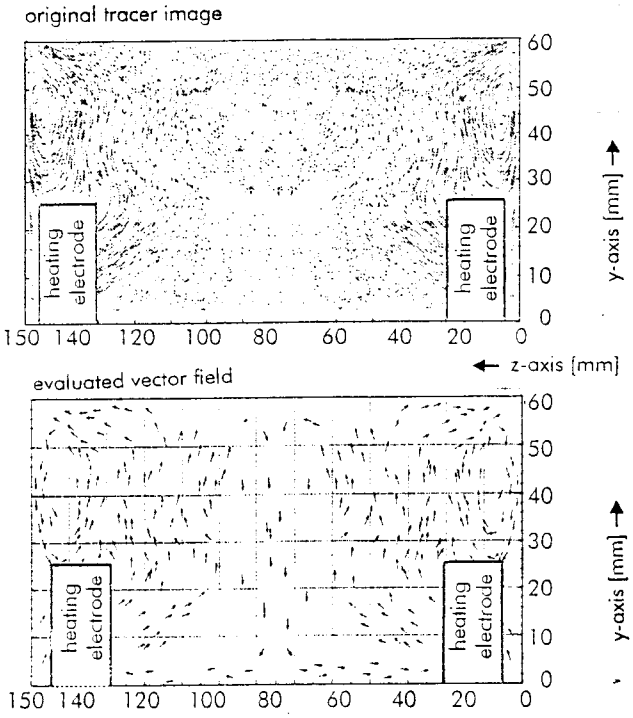

FIGURE 30: FLOW FIELD IN GLASS MELT TUB
CROSS SECTION OF MELTING REGION

different times can be done by means of the trajectories. This means in practical use, that in a first step the trajectory of a tracer particle is determined. In the second step the image processing system will search the other single images for pixels which fit to this special trajectory. Using this method, the pixels belonging together can be found with a very high reliability.

Figure 29 shows the experimental set-up of the tub. The model is made of glass to allow optical access. In the following only the melting region is observed. To get as close as possible to properties of matter of the glass melt a water-acrylic resin-soda lye mixture was used as model fluid. The heating was realized by 12 copper electrodes. The flow of the glass melt within the tub results from a superposition of the convective flow and of the tapping flow. With the knowledge of the flow field the tube geometry and electrodes arrangement can be optimized (Götz, 1995).

Lancet Tube Bundle

The performance of a tube bundle heat exchanger can be improved by giving the tubes special shapes (figure 31) This lancet shape brings two big advantages compared to the common circular tubes: 1. larger heat transfering surface 2. smoother changes in the free cross sectional area between tube rows. In figure 30 the temperature field (holographic interferogram) in the tube bundle is presented. The figure 32 shows the local Nusselt number over the perimeter of lancets from the 2nd tube row (Mayinger and Fehle, 1994).

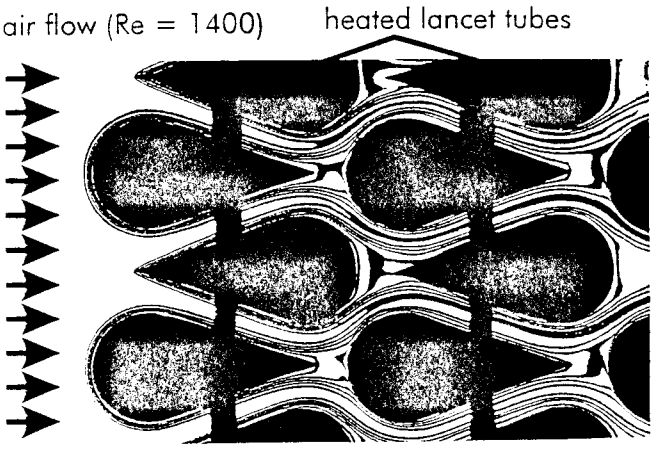

FIGURE 31: TEMPERATURE FIELD IN LANCET BUNDLE

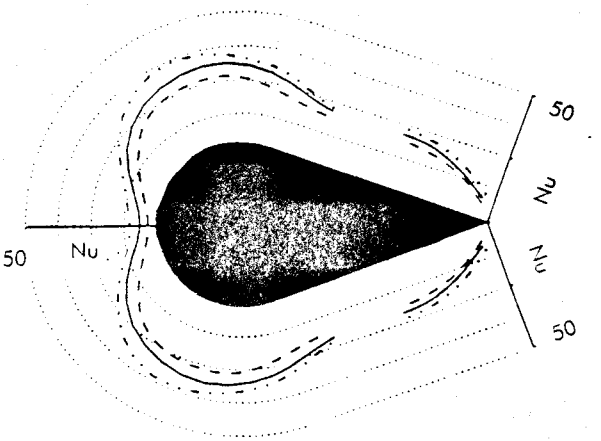

FIGURE 32: LOCAL NUSSELT NUMBER OVER THE PERIMETER OF LANCETS FROM THE 2nd TUBE ROW

Impinging Jets for the Drying of Varnished Paper

Object of the investigation is the drying section of a varnishing machine built up of convective and radiative modules. The convective module consists either of a slot nozzle array or of a round nozzle array. One goal of the investigations is the optimization of the nozzle's geometry and their geometrical arrangement within the given area.

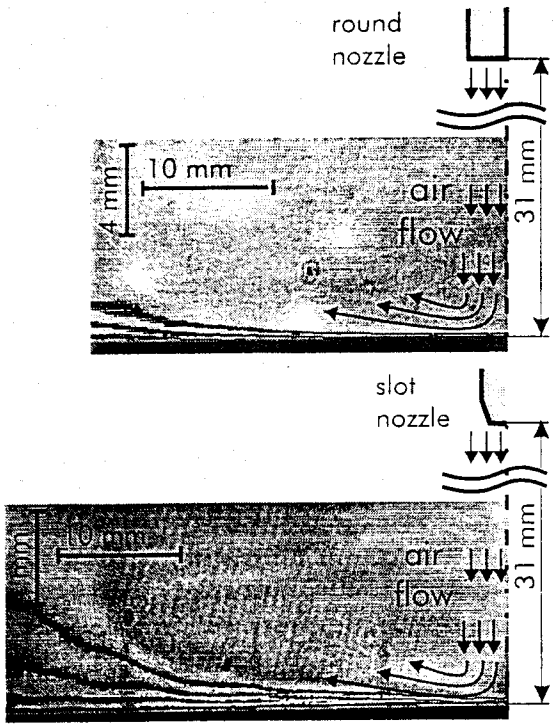

FIGURE 33: TEMPERATURE FIELD OF JET FLOW

Figure 33 shows interferograms of the thermal boundary layer of an air flow emerging either from a round nozzle or a slot nozzle. Both pictures have been taken at an equal air volume flow per drying area (0.082 m^3/m^2s). One can see the much higher temperature gradient at the upper image which shows a higher heat transfer coefficient at this nozzle arrangement. This behaviour results from the higher outlet flow velocities from the round nozzles (Mintzlaff, 1997).

CONCLUDING REMARKS

New highly intensified cameras (CCD) with a very high temporal resolution together with computer aided evaluation of images arise new challenges for measurements and can help to find a better understanding of transport phenomena in heat transfer and fluiddynamics. The practical examples presented above show that it is possible to obtain detailed thermohydraulic informations for a wide range of different applications with the modern optical methods described in the first part.

REFERENCES

Andresen, P., et al., 1990, "Fluorescence imaging outside an internal combustion engine using tunable excimer lasers", *Applied Optics*, Vol. 29, No. 16

Andresen, P., et al., 1992, "Identifcation and imaging of OH and O2 in an automobile spark-ignition engine using a tunable KrF excimer laser", *Applied Optics*, Vol. 29, No. 16

Chavez, A., 1991, "Holographische Untersuchung an Einspritzstrahlen: Fluiddynamik und Wärmeübergang durch Kondensation", Diss., Technical University of Munich

Chavez, A., and Mayinger, F., 1992, "Measurement of the direct-contact condensation of pure saturated vapour on an injection spray by applying pulsed laser holography", *Int. J. Heat Mass Transfer*, Vol. 35, No. 3, pp. 691-702

Chen Y.M., et al., 1991, "Heat Transfer at the Phase Interface of Condensing Bubbles", Phase-interface Phenomena in Multiphase Flow, Eds.: Hewitt, G.F. et al., Hemisphere, New York, pp. 433-442

Chen, Y.M., 1985, "Wärmeübergang an der Phasengrenze kondensierender Blasen", Diss., Technical University of Munich

Durst, F., 1987, "Theorie und Praxis der Laser-Doppler-Anemometrie", G.Braun Verlag, Karlsruhe

Eckbreth, A.C., 1988, "Laser Diagnostics for Combustion Temperature and Species", Abacus Press, Tunbridge Wells, UK

Fehle, R., and Mayinger, F., 1996, "Enhancement of forced convection cooling of highly loaded heat sources in a rectangular channel by flow deflectiony", *Proc., 9th International Symposium on Transport Phenomena in Thermal-Fluids Engineering*, Vol. 1, pp.663-668, Singapore

Feldmann, O., et al., 1997, "Evaluation of Pulsed Laser Holograms of Flashing Sprays by Digital Image Processing and Holographic Particle Image Velocimetry", Proc., CSNI Specialist Meeting on Advanced Instrumentation, Santa Barbara, USA

Gabor, D., 1951, "Microscopy by Reconstructed Wavefronts II", *Proc. Roy. Soc.*, B64, London

Gebhard, P., and Mayinger, F., 1996, "Evaluation of Pulsed Laser Holograms of Flashing Sprays by Digital Image Processing", *Flow Visualization and Image Processing of Multiphase Systems*, ASME, FED-Vol. 209

Götz, W., 1995, "Thermo-fluiddynamische Vorgänge in Glasschmelzwannen", Diss., Technical University of Munich

Hauf, W., and Grigull, U., 1970, "Instationärer Wärmeübergang durch freie Konvektion in horizontalen Zylindern", *Int. Conf. Heat Transfer*, 4 , Versailles

Hauf, W., et al., F., 1991, "Optische Meßverfahren in der Wärme- und Stoffübertragung", Springer-Verlag, Berlin

Kiemle, H., and Röss, D., 1969, "Einführung in die Technik der Holografie", Akademische Verlagsgesellschaft, Frankfurt a.M.

Mayinger, F.(ed.), 1994, "Optical Measurements", Springer Verlag, Berlin

Mayinger, F., and Fehle, R., 1994, "Bestimmung des Temperaturfeldes in Kompakt-Wärmetauschern mit Hilfe der holographischen Interferometrie", Chair A for Thermodynamics, Technical University of Munich

Mayinger, F., and Panknin, W., 1974, "Holography in Heat and Mass Transfer", *5th Int.Heat Transfer Conf.*, VI, 28-43, Tokio

Mayinger, F., et. al., 1993, "Structure and Burning Velocity of Premixed, Turbulent Hydrogen-Air-Flames", Proc., *ICHMT Int. Symp. (Energy Systems and Environmental Effects)*, Cancun, Mexico

Mintzlaff, J., and Mayinger, F., 1997, "Drying of Water-based Varnishes", Chair A for Thermodynamics handout, Technical University of Munich

Panknin W., and Mayinger, F., 1978, "Anwendung der holographischen Zweiwellenlängeninterferometrie zur Messung überlagerter Temperatur- und Konzentrationsgrenzschichten, *Verfahrenstechnik*, Bd. 12,9, pp. 582-589

Tauscher, R., and Mayinger, F., 1997, "Enhancement of Heat Transfer in a Plate Heat Exchanger by Turbulence Promotors", *Proc.,Heat Exchangers for the Process Industries*, Snowbird, USA